Journal of Veterinary Science

JVS

Original Article
Toxicology

Check for updates

Hepatotoxic mechanism of diclofenac sodium on broiler chicken revealed by iTRAQ-based proteomics analysis

Chuanxi Sun [1,2], **Tianyi Zhu** [1], **Yuwei Zhu** [1], **Bing Li** [1], **Jiaming Zhang** [1], **Yixin Liu** [1], **Changning Juan** [1], **Shifa Yang** [2,3], **Zengcheng Zhao** [2,3], **Renzhong Wan** [1,*], **Shuqian Lin** [2,3,*], **Bin Yin** [2,3,*]

[1]College of Animal Science and Veterinary Medicine, Shandong Agricultural University, Taian 271018, China
[2]Institute of Poultry Science, Shandong Academy of Agricultural Sciences, Jinan 250100, China
[3]Shandong Provincial Animal and Poultry Green Health Products Creation Engineering Laboratory, Jinan 250100, China

OPEN ACCESS

*Corresponding authors:

Renzhong Wan

College of Animal Science and Veterinary Medicine, Shandong Agricultural University, 61 Daizong Road, Taian 271018, China.
Email: wrzh63@163.com
https://orcid.org/0000-0003-4755-0715

Shuqian Lin

Institute of Poultry Science, Shandong Academy of Agricultural Sciences, 202 Gongyebei Road, Jinan 250100, China.
Email: shuqianlin@126.com
https://orcid.org/0000-0001-7134-022X

Bin Yin

Institute of Poultry Science, Shandong Academy of Agricultural Sciences, 202 Gongyebei Road, Jinan 250100, China.
Email: yb53650@163.com
https://orcid.org/0000-0002-4572-7735

ABSTRACT

Background: At the therapeutic doses, diclofenac sodium (DFS) has few toxic side effects on mammals. On the other hand, DFS exhibits potent toxicity against birds and the mechanisms remain ambiguous.

Objectives: This paper was designed to probe the toxicity of DFS exposure on the hepatic proteome of broiler chickens.

Methods: Twenty 30-day-old broiler chickens were randomized evenly into two groups (n = 10). DFS was administered orally at 10 mg/kg body weight in group A, while the chickens in group B were perfused with saline as a control. Histopathological observations, serum biochemical examinations, and quantitative real-time polymerase chain reaction were performed to assess the liver injury induced by DFS. Proteomics analysis of the liver samples was conducted using isobaric tags for relative and absolute quantification (iTRAQ) technology.

Results: Ultimately, 201 differentially expressed proteins (DEPs) were obtained, of which 47 were up regulated, and 154 were down regulated. The Gene Ontology classification and Kyoto Encyclopedia of Genes and Genomes pathway analysis were conducted to screen target DEPs associated with DFS hepatotoxicity. The regulatory relationships between DEPs and signaling pathways were embodied via a protein-protein interaction network. The results showed that the DEPs enriched in multiple pathways, which might be related to the hepatotoxicity of DFS, were "protein processing in endoplasmic reticulum," "retinol metabolism," and "glycine, serine, and threonine metabolism."

Conclusions: The hepatotoxicity of DFS on broiler chickens might be achieved by inducing the apoptosis of hepatocytes and affecting the metabolism of retinol and purine. The present study could provide molecular insights into the hepatotoxicity of DFS on broiler chickens.

Keywords: Diclofenac sodium; chicken; toxicity; liver; proteomics

INTRODUCTION

Diclofenac sodium (DFS) is considered one of the most widely used non-steroidal anti-inflammatory drugs (NSAIDs) owing to its preeminent analgesic, anti-inflammatory, and antipyretic activities [1]. Clinically, DFS is used extensively for rheumatoid arthritis (RA),

Generated by xmlinkpress

ORCID iDs
Chuanxi Sun
https://orcid.org/0000-0002-2009-3799
Tianyi Zhu
https://orcid.org/0000-0001-7690-280X
Yuwei Zhu
https://orcid.org/0000-0002-3015-9181
Bing Li
https://orcid.org/0000-0002-5113-8435
Jiaming Zhang
https://orcid.org/0000-0003-4820-7329
Yixin Liu
https://orcid.org/0000-0001-6824-355X
Changning Juan
https://orcid.org/0000-0002-6326-9301
Shifa Yang
https://orcid.org/0000-0002-2551-9189
Zengcheng Zhao
https://orcid.org/0000-0002-9565-3770
Renzhong Wan
https://orcid.org/0000-0003-4755-0715
Shuqian Lin
https://orcid.org/0000-0001-7134-022X
Bin Yin
https://orcid.org/0000-0002-4572-7735

ankylosing spondylitis (AS), osteoarthritis (OA), postoperative pain, and fever of various origins [2]. DFS is a non-selective inhibitor of the cyclooxygenase (COX, type 1 and 2), which can prevent the conversion of arachidonic acid to prostaglandins (PGs) by inhibiting the activity of cyclooxygenase [3]. In contrast to conventional NSAIDs, DFS has the characteristics of rapid onset, strong efficacy, and low side effects rate [4].

DFS has few severe toxic side effects on mammals at therapeutic doses, but DFS is lethal to birds. The oral median lethal dose (LD_{50}) of DFS was higher than 200 mg/kg in rats but only 0.1–0.2 mg/kg in vultures [5,6]. Reports on the drastic reduction of vulture populations caused by DFS residues in the Indian subcontinent have attracted attention [7,8]. Hence, to preserve the vultures, DFS has been banned in veterinary medicine within this region and replaced with other alternative NSAIDs, such as meloxicam [9,10]. Subsequent studies have reported that DFS could cause significant toxicity in various birds with primary manifestations of severe liver and kidney injury and widespread deposition of urate crystals [11]. Currently, most studies on the toxic mechanism of DFS on bird species were in terms of its nephrotoxicity. Some studies suggested that the primary cause of the toxic effects of DFS in birds is kidney damage, which in turn blocks the excretion of uric acid [12,13]. A previous study on the nephrotoxicity of DFS on broiler chickens used isobaric tags for relative and absolute quantification (iTRAQ)-based proteomics [14]. The present study examined the hepatotoxic mechanism.

Proteomics could explore the mechanism of different drugs and the pathogenesis of diseases from the protein perspective [15]. iTRAQ is a multiplex labeling technology for quantifying proteins based on tandem mass spectrometry [16]. iTRAQ technology is an effective tool to compare the proteome alterations between the different biological samples by labeling proteins with isobaric tags. All the proteins in the samples could be analyzed qualitatively and quantitatively, and the differentially expressed proteins (DEPs) were identified.

This study examined the toxicity of DFS exposure on the hepatic proteome of broiler chicken. The proteins in the liver samples were characterized and quantified via iTRAQ technology after the oral administration of DFS (10 mg/kg body weight). Gene Ontology (GO) function and Kyoto Encyclopedia of Genes and Genomes (KEGG) pathway analysis of the identified DEPs were performed. The biological networks that may be affected by these DEPs were then exhibited through a protein-protein interaction (PPI) network. This study has set the stage for further research to explain the hepatotoxic mechanism of DFS on broiler chickens.

MATERIALS AND METHODS

Animal grouping and dosing regimen
Twenty broiler chickens (30 days old) were purchased from a commercial hatchery (China). The chickens were reared in the isolator with access to food and water *ad libitum*. After acclimatization for two weeks, the chickens were randomized into two groups (n = 10) and fasted for one night before the experiment with free access to water. DFS was administered at 10 mg/kg body weight through a gavage in group A [11,17,18], while the chickens in group B were perfused with saline as a control. The chickens were observed after administration, and they were euthanized after 48 h except for the toxic deaths. All animal procedures were approved by the Institutional Animal Care and Use Committee of the Shandong Academy of Agricultural Sciences (SAAS-2019-032).

Serum biochemical examination

Blood was obtained from the wing vein before and at four and 10 h after DFS administration, and the serum was isolated. The alanine aminotransferase (ALT) and aspartate aminotransferase (AST) activities were included as the biochemical indicators of hepatic damage, and the uric acid content in serum was also measured simultaneously. All the detection kits were supplied by Jiancheng Bioengineering Institute (Nanjing, China).

Histopathology

The liver samples were collected separately and immersed immediately in a fixative (4% paraformaldehyde). After fixation, the tissues were then embedded in paraffin and sliced. Afterward, sections were stained with hematoxylin-eosin (H&E) for the histopathological examinations.

Expression of apoptosis-related genes

The expression of three apoptosis-related genes (*Bax*, *Bcl-2*, and *caspase 3*) was evaluated using a quantitative real-time polymerase chain reaction (qRT-PCR) to reveal the liver injury. Liver tissue homogenates were prepared under cryogenic conditions, and the total RNA was isolated via RNAios Plus (TaKaRa, Japan). The purity and quantity of RNA were calculated with a NanoDrop 2000 spectrophotometer (Thermo Fisher Scientific, USA). Evo M-MLV RT Kit (Accurate Biotechnology, China) was utilized to generate cDNA. After the reverse transcription, qRT-PCR was performed with PerfectStart™ Green qPCR SuperMix (TransGen Biotech, China). Glyceraldehyde-3-phosphate dehydrogenase (GAPDH) was defined as the housekeeping gene, and the comparative Ct ($2^{-\Delta\Delta Ct}$) method was used to calculate the relative transcript level of target genes. **Table 1** lists the primer sequences.

Table 1. qRT-PCR primer sequences

Gene name		Primer sequence	Product length (bp)
GAPDH	Forward	5'-TGAAAGTCGGAGTCAACGGAT-3'	191
	Reverse	5'-ACGCTCCTGGAAGATAGTGAT-3'	
Bcl-2	Forward	5'-CTCTTCCGTGATGGGGTCAA-3'	188
	Reverse	5'-ACAAAGGCATCCCATCCTCC-3'	
Bax	Forward	5'-AACCCCAGCATTATCCCCAC-3'	200
	Reverse	5'-ACGTACAGATTGGCCGTGAA-3'	
Caspase 3	Forward	5'-TGCTCCAGGCTACTACTCCT-3'	90
	Reverse	5'-TTCCTGGCGTGTTCCTTCAG-3'	
CYP3A5	Forward	5'-GGAATACCTCGACATGGCCG-3'	70
	Reverse	5'-GGTTCTCTCAAGCCGTCCTC-3'	
HSPA5	Forward	5'-GGTGTTGCTTGATGTGTGTCC-3'	190
	Reverse	5'-ATGATTGTCCTTGGTGAGGGG-3'	
CALR	Forward	5'-TCCGCTGCAAGGATGATGAG-3'	103
	Reverse	5'-CTCCCCGATTCCACTTTGCT-3'	
STUB1	Forward	5'-GCGGATCAACCAAGAGAACG-3'	189
	Reverse	5'-AAGAGTTCATCCATGTCTGCCA-3'	
CYP3A4	Forward	5'-CCCCGTCCTCATCAAAACCA-3'	79
	Reverse	5'-CCCACTCAGACCAAAGACCC-3'	
TDH	Forward	5'-CGGACACACGCCTTCCTATG-3'	124
	Reverse	5'-GGAGTGAAGCTCATGGCACT-3'	
LOC101747660	Forward	5'-GAGGACCCCACGGTCAATG-3'	80
	Reverse	5'-GCTGTGGGTACAAAAAGGGC-3'	
GATM	Forward	5'-CCTGACTACCGAGTGCATGT-3'	127
	Reverse	5'-CCCACTCAGACCAAAGACCC-3'	
CYP2C45	Forward	5'-TTTGTGTTGCTTGCCTGCTC-3'	181
	Reverse	5'-AGTTGCACTGAGAAGACGGG-3'	

qRT-PCR, quantitative real-time polymerase chain reaction; GAPDH, glyceraldehyde-3-phosphate dehydrogenase.

Proteomics studies

Preparation of protein samples

The livers used for proteomic analysis were harvested after sampling and transferred immediately in liquid nitrogen until extraction. The proteins were extracted with a lysis buffer consisting of 1 × Protease Inhibitor Cocktail (Roche Ltd., Switzerland), 1% sodium dodecyl sulfate, and 8 M urea. The lysates were vibrated and ground three times for 400 sec each. After completing the lysis for 30 min on ice, the supernatants were split off via centrifugation at 15,000 rpm at 4°C for 30 min and then harvested.

Digestion of the proteins and iTRAQ labeling

After the measurements using the BCA assay kit, 100 μg protein in the supernatant of the individual sample was aspirated into a new EP tube, and the volume was brought to 100 μL by urea (8 M). Subsequently, 2 μL TCEP (0.5 M) was added to each tube, and the proteins were incubated at 37°C. After 1 h, the sample was treated with 4 μL iodoacetamide (1 M), followed by an additional reaction for 40 min at room temperature (protected from light). The samples were precipitated with five volumes of pre-chilled acetone overnight at −20°C. The mixture was centrifuged at 12,000 g at 4°C for 20 min, and the precipitate was ultimately retained. Subsequently, the precipitate was cleaned twice with 90% pre-chilled acetone and dissolved in 100 μL of TEAB (100 mM) after the complete evaporation of acetone. Trypsin (Promega, Madison, WI) was added to the redissolved sample for overnight digestion at 37°C based on the 1:50 mass ratio (trypsin: protein). Before lyophilization, the digested peptides were desalted with a ZipTip C18 column and quantified using a peptide quantification kit (Pierce 23275). Labeling of the peptides was performed using an iTRAQ-8plex Isobaric Mass Tag Labeling Kit (Thermo Fisher Scientific). Finally, the labeled peptides were mixed and lyophilized again.

High pH reverse phase separation

The lyophilized iTRAQ-labeled peptides were dissolved in buffer A (20 mM aqueous solution of ammonium formate, adjusted to pH 10 with ammonia). The high pH fractionation was performed using an Ultimate 3000 system (Thermo Fisher Scientific) equipped with an XBridge C18 reverse-phase column (250 mm × 4.6 mm, 5 μm particle size; Waters Corporation, USA). A linear gradient from 5% to 45% buffer B (20 mM ammonium formate in 80% ACN, adjusted with ammonia to pH 10) over 40 min was used. The column temperature was 30°C while the flow rate of the mobile phase was maintained at 1.0 mL/min. The reverse-phase column was equilibrated for 15 min under initial conditions. Eventually, 10 fractions were obtained and dried using a vacuum concentrator.

Nano-HPLC-MS/MS analysis

After redissolved respectively in 30 μL solvent A (0.1% aqueous solutions of formic acid), LC-MS/MS analysis of the salt-free lyophilized peptides was conducted using an Orbitrap Fusion Mass Spectrometer connected in series to an EASY-nLC 1200 system (Thermo Fisher Scientific). These peptides were loaded onto an Acclaim PepMap C18 analytical column (15 cm × 75 μm). The separation was achieved by a linear gradient from 6% to 45% solvent B (0.1% formic acid in ACN) over 60 min. The mobile phase was set with a 0.3 mL/min flow rate while the column temperature was 40°C. The sample injection volume was 3 μL, and the electrospray voltage was 2.0 kV.

The parameters for Orbitrap Fusion mass spectrometer were as follows: (1) MS: scan range (m/z) = 375–1,800; resolution = 60,000; AGC target = 5e5; maximum injection time = 50 ms;

include charge states = 2–6; dynamic exclusion = 30 sec; (2) HCD-MS/MS: resolution = 15,000; AGC target = 5e4; isolation window = 2; maximum injection time = 50 ms; collision energy = 38.

Data and bioinformatics analysis
PEAKS studio X+ (Bioinformatics Solutions Inc., Canada) was used to assess the mass spectra data, and PEAKS DB was used to search the "Gallus_gallus_201907.fasta" protein database. "Trypsin" was defined as the proteolytic enzyme with up to two missed cleavages allowed. The mass error tolerances were set to 7 ppm for parent ions and 0.02 Da fragment ions, respectively. Itraq 8plex (K, N-term) 304.20 and carbamidomethylation (C) 57.02 were specified as the fixed modifications, while acetylation (Protein N-term) 42.01, oxidation (M) 15.99 and deamidation (NQ) 0.98 were variable modifications. A 1% false discovery rate (FDR) and one unique peptide were applied to filter the peptides. The DEPs were defined using the following criteria: over 1.2-fold change, $p <$ 0.05, and at least one unique peptide (according to the analysis of variance [ANOVA] algorithm).

The distribution of up- and down-regulated DEPs were visualized using a volcano plot depicted using the ggplot2 package (http://ggplot2.org). Functional enrichment and annotation analyses of DEPs were carried out by GOATOOLS and Blast2GO version 5, respectively. A webserver KOBAS (http://kobas.cbi.pku.edu.cn/) was used to implement KEGG analysis. The interactions among the DEPs were displayed using a PPI network, which was generated via STRING v11.5 (www.string-db.org).

Verification of the proteomic results
The expression of genes corresponding to screened DEPs was evaluated by qRT-PCR. The specific operation steps were carried out in reference to "Expression of apoptosis-related genes". **Table 1** also lists the primer sequences.

Statistical analysis
All parametric data were subjected to one-way ANOVA followed by a least significance difference (LSD) test for multiple comparisons. The p values < 0.05, < 0.01, and < 0.001 were considered statistically significant.

RESULTS

Serum biochemical examination
Fig. 1 shows the assay results of serum biochemical indicators. The AST activity in the serum of broiler chickens increased significantly after DFS administration compared to the control group (**Fig. 1B**). Although no significant difference in the ALT activity was detected, the bar plot still showed an increasing trend (**Fig. 1A**). The uric acid content was also elevated significantly in the DFS-administered group within a short period (**Fig. 1C**).

Histopathology
Chickens in the DFS-administered group began to die with the apparent symptoms of poisoning after oral gavage administration for a period. The necropsy of the dead chickens showed that the liver was enlarged with the deposition of white urate on the surface. In contrast, there was no manifestation of poisoning in the control group, and no abnormality was detected at necropsy. Compared to the control group, the histopathological changes in the liver sections consisted of dilatation of the hepatic sinusoids and focal necrosis with inflammatory cell infiltration. **Fig. 2** shows the aforementioned changes.
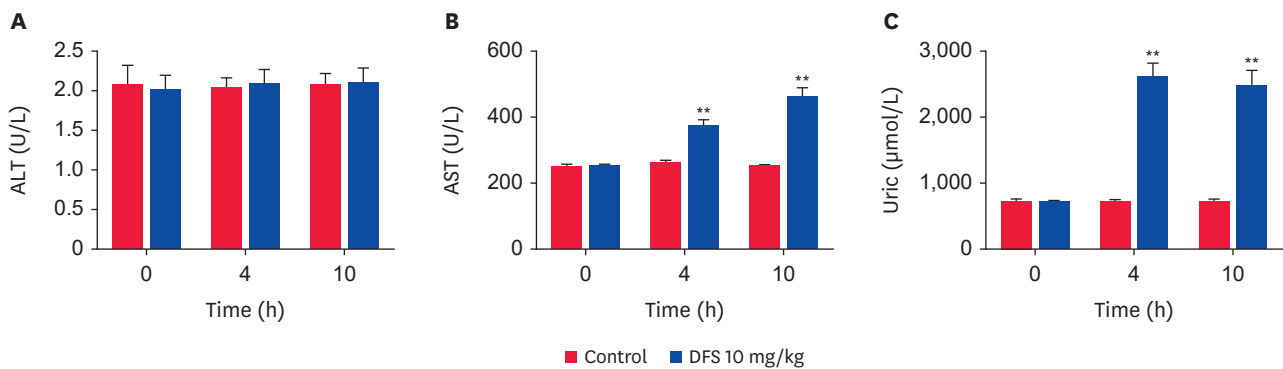
Fig. 1. Results of the serum biochemical examination presented via bar plots.
(A) Activity of ALT for different periods after DFS administration; (B) Activity of AST for different periods after DFS administration; (C) The content of uric acid in serum for different periods. The data are presented as mean ± SEM.
AST, aspartate aminotransferase; DFS, diclofenac sodium; ALT, alanine aminotransferase; SEM, standard error of the mean.
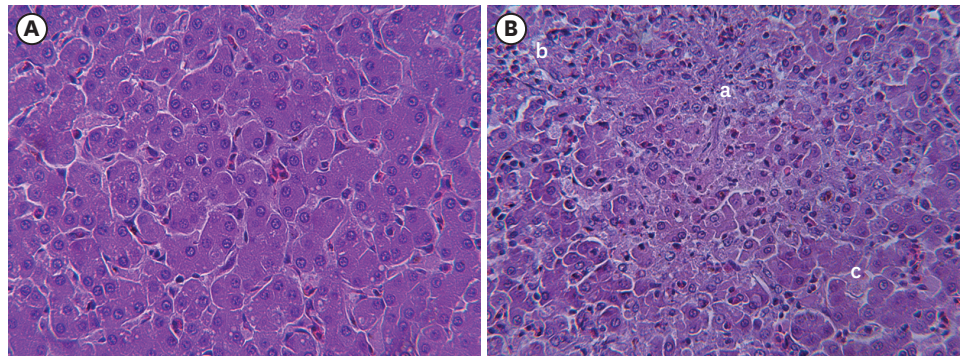*$p < 0.05$, **$p < 0.01$.

Fig. 2. H&E stained histopathology sections of the liver. (A) Normal liver section from the control group, H&E ×400. (B) Liver section from dosed chickens that succumbed, H&E ×400. Focal hepatic necrosis (a), inflammatory cell infiltration (b), and dilatation of hepatic sinusoids (c).
H&E, hematoxylin-eosin

Expression of apoptosis-related genes

Fig. 3 shows the mRNA transcript levels of apoptosis-related genes in the liver. After the oral administration of DFS (10 mg/kg), mRNA transcript levels of *Bax* ($p < 0.01$) and *caspase 3* ($p < 0.01$) were up regulated significantly, while *Bcl-2* ($p < 0.01$) was down-regulated significantly. *Bcl-2* could inhibit apoptosis, while *Bax* could antagonize the inhibition of *Bcl-2* and induce apoptosis. Caspase activation is considered the hallmark of apoptosis, and *caspase 3* is the most important member in the apoptotic endpoint [19,20]. This study hypothesized that DFS induces liver cell apoptosis by enhancing the mRNA transcript levels of pro-apoptotic genes and simultaneously suppressing the transcript levels of the anti-apoptotic genes.

Protein identification

In the present study, the information obtained by iTRAQ technology was aligned and compared with the database, and 4,221 proteins were identified. The peptides were predominantly between nine and 19 amino acids in length (**Fig. 4A**). The reasonable peptide length distribution indicated the relatively high quality of data. Seven hundred and ninety-four proteins had more than 10 peptides, while others contained 1–10 peptides (**Fig. 4B**). The proportion of the relative molecular weight of proteins greater than 100 kDa was 15.80%, and the rest of the proteins ranged from zero to 100 kDa (**Fig. 4C**). The protein sequence coverage of 0–10%, 10–20%, 20–30%, 30–40%, and 40–100% accounted for 41.07%, 20.30%, 14.45%, 9.55%, and 13.93%, respectively (**Fig. 4D**).
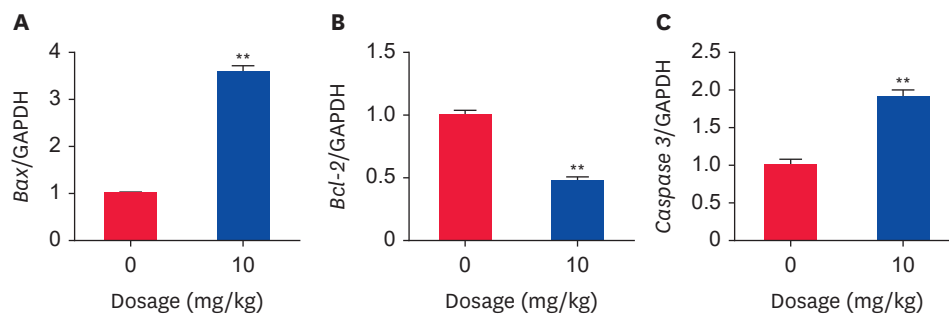
Fig. 3. Effects of DFS on the apoptosis-related genes.
(A) Relative mRNA expression level of *Bax*; (B) Relative mRNA expression level of *Bcl-2*; (C) Relative mRNA expression level of *caspase 3*. Data are presented as mean ± SEM.
DFS, diclofenac sodium; SEM, standard error of the mean; GAPDH, glyceraldehyde-3-phosphate dehydrogenase.
*$p < 0.05$, **$p < 0.01$.

Fig. 4. Identification results of the proteins. (A) Peptide length distribution; (B) Peptide number distribution; (C) Peptide mass distribution; (D) Protein sequence coverage. The identification results of the proteins suggested the high quality of data.

https://doi.org/10.4142/jvs.22018

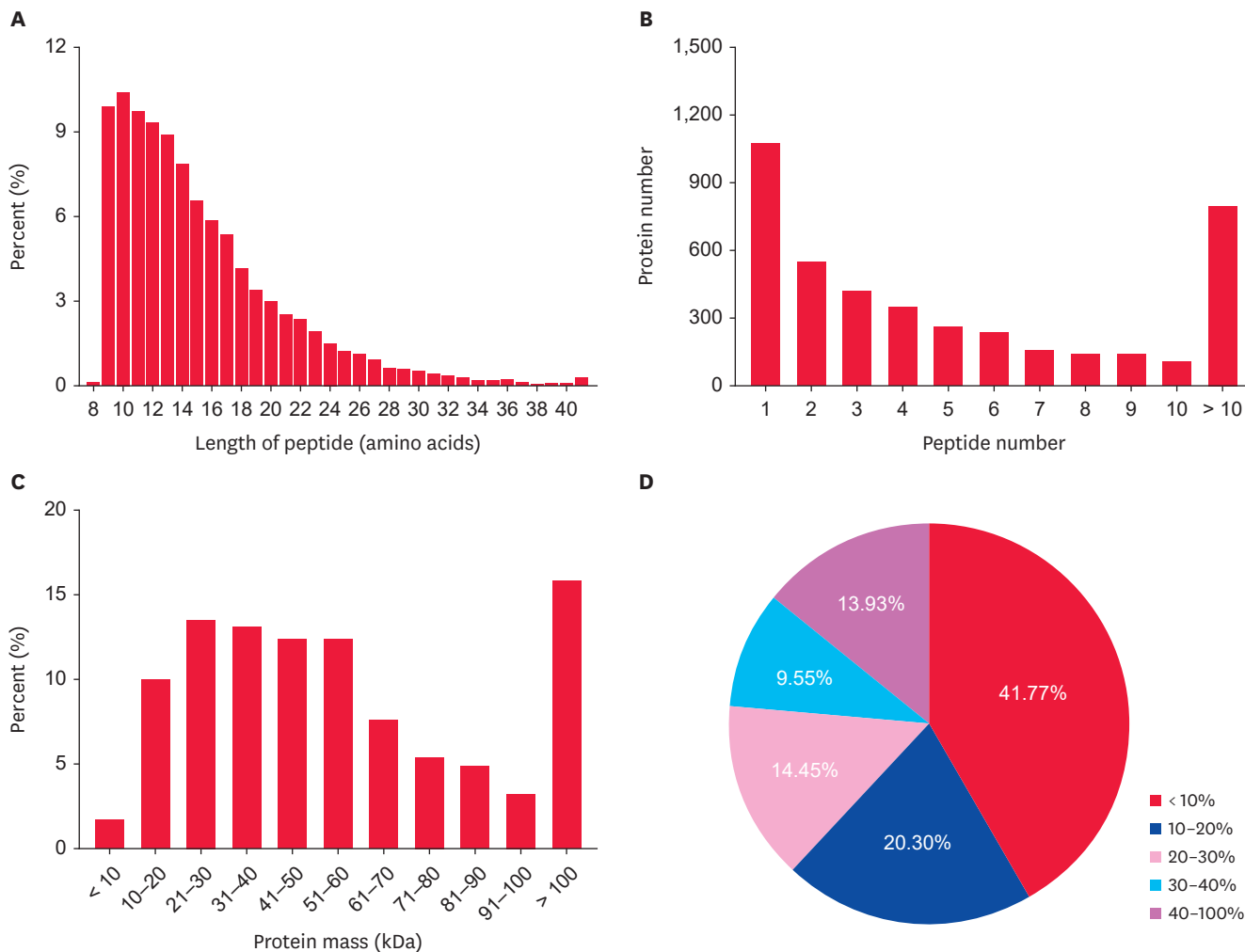### Identification of DEPs

As shown in **Fig. 5**, a volcano plot was used to demonstrate the distribution of DEPs. The screening criteria for DEPs were as follows: fold change ≥ 1.2 or ≤ −1.2; at least 1 unique peptide; $p < 0.05$ by ANOVA. Two hundred and one DEPs were obtained. Among those, 154 were down regulated, and 47 were up-regulated. The top 10 down-regulated and 10 most up-regulated DEPs were identified based on the fold change (**Table 2**). ACTBL2 was the most down-regulated DEPs in the liver with a 2.84-fold change, and S100A9 was the most up-regulated DEPs with a 2.36-fold change.

GO enrichment for DEPs

DEPs in the enrichment results under three classifications (biological process, cellular component, and molecular function) were sorted according to the p value. The number of DEPs with the smallest p values in the top 20 GO terms (level 2) were counted. As shown in **Fig. 6**, three pie charts were plotted to show the proportion of the number of DEPs in each term.

Within the biological process category, "organic substance metabolic process," "nitrogen compound metabolic process," "primary metabolic process," "cellular metabolic process," "response to stress," and "catabolic process" were mainly enriched, accounting for 17.53%, 16.16%, 15.62%, 15.07%, 6.58%, and 5.21%, respectively. Under the cellular component category, DEPs are enriched considerably in the "membrane-bounded organelle,"
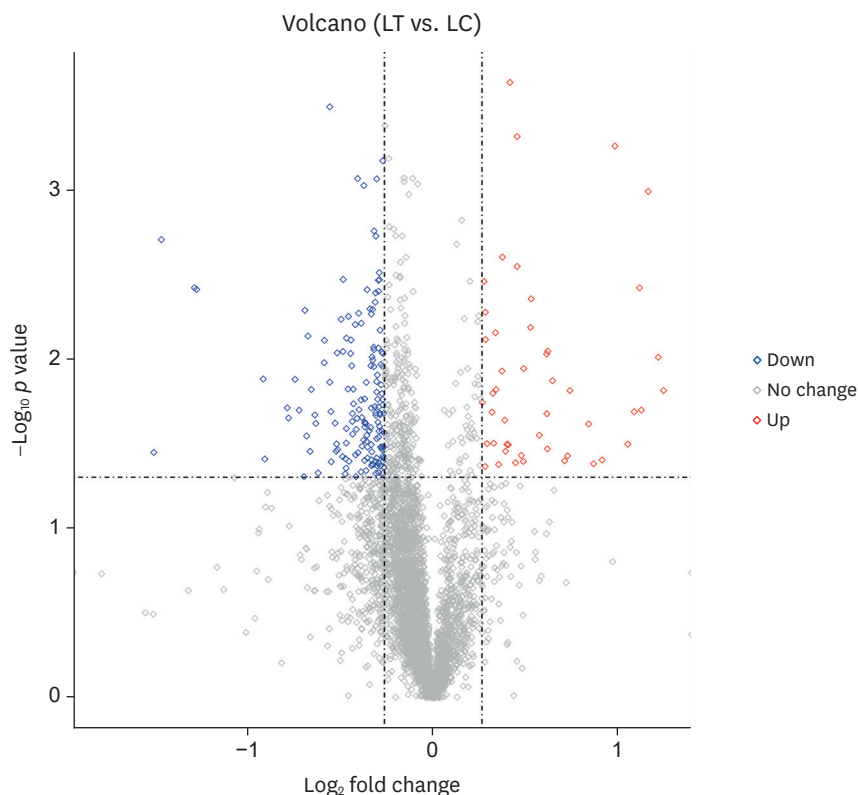
Fig. 5. Volcano plot generated with the fold change ($\log_2$ transformed) as a horizontal coordinate and p value ($−\log_{10}$ transformed) as the vertical coordinate. Based on the threshold of significance ($p < 0.05$), the data were classified into three categories: the blue dots indicate down-regulated DEPs, red dots correspond to up-regulated DEPs, and grey dots mean no significant differential expression.
DEP, differentially expressed protein; LT, livers from treated group; LC, livers from control group.

Table 2. Top 10 up-regulated and down-regulated DEPs

Accession	Description	Gene name	Fold change	p value
P28318	Protein MRP-126	S100A9	+2.36	0.015452544
P80389	Antimicrobial peptide CHP1	AvBD1	+2.32	0.009840111
F1NT18	Cytochrome P450 3A5	CYP3A5	+2.23	0.001035142
P02001	Hemoglobin subunit alpha-D	HBAD	+2.18	0.020137242
Q6QLQ9	Gallinacin-10	GAL10	+2.16	0.003828247
P02112	Hemoglobin subunit beta	HBB	+2.12	0.020606299
P01994	Hemoglobin subunit alpha-A	HBAA;	+2.07	0.031988951
F1NK40	Uncharacterized protein	A2ML4	+1.97	0.00055847
Q6QLR3	Gallinacin-6	GAL6	+1.88	0.039627803
A0A1D5PHX5	ER lumen protein-retaining receptor	KDELR3	+1.82	0.041783037
E1BZY3	Gamma-glutamylaminecyclotransferase	GGACT	−1.58	0.035318317
E1BS56	SERPIN domain-containing protein	SERPINA4	−1.60	0.007379042
A0A1D5P0Y1	O-GlcNAc transferase subunit p110	OGT	−1.62	0.00519996
A0A1D5PJV0	Host cell factor 2	HCFC2	−1.62	0.049773708
P07322	Beta-enolase	ENO3	−1.65	0.020183664
E1BZE1	Alpha-2-HS-glycoprotein	AHSG	−1.68	0.013273945
A0A1D5PY49	Histone H2B	LOC426037	−1.88	0.039174188
P81476	Ribonuclease CL2	CL2	−2.44	0.003828247
A0A1D5PKQ8	Cytochrome P450 2C45	CYP2C45	−2.76	0.001990673
A0A1D5NV17	Beta-actin-like protein 2	ACTBL2	−2.84	0.035809644

Plus and minus values of fold change represent the up- and down-regulated alteration trend of DEPs, respectively.
DEP, differentially expressed protein.

"extracellular organelle," "extracellular space," and "extracellular matrix," accounting for 37.67%, 20.55%, 13.70%, and 6.85%, respectively. For the molecular function category, the predominantly enriched terms are "ion binding," "hydrolase activity," "enzyme regulator activity," and "cofactor binding," accounting for 44.30%, 22.15%, 7.38%, and 6.71%, respectively. The DEPs in these GO terms might be closely associated with the hepatotoxicity of DFS towards broiler chicken.

KEGG analysis for DEPs and selection of the target DEPs

Pathways with corrected p values (Benjamini and Hochberg algorithm) less than 0.05 were considered significant, and the results were visualized from a bar plot in **Fig. 7**. Ordered by the proportion of DEPs, the most significant enrichment pathway is "metabolic pathways." Other pathways included "protein processing in endoplasmic reticulum," "retinol metabolism," "steroid hormone biosynthesis," "ECM-receptor interaction," "linoleic acid metabolism," "drug metabolism-cytochrome P450," "metabolism of xenobiotics by cytochrome P450," "glycine, serine, and threonine metabolism," "RNA degradation," "protein export," "drug metabolism-other enzymes," and "starch and sucrose metabolism." These pathways mentioned above were the focus of the following studies to explore the mechanism of DFS hepatotoxicity towards broiler chickens.

The liver is a crucial metabolic organ, and the expression of DEPs was predominantly found in several metabolism-related pathways based on GO and KEGG analysis. **Table 2** lists some screened DEPs that might be associated with the hepatotoxicity of DFS towards broiler chickens. As indicated in **Fig. 8**, the STRING database (v11.5) was utilized to establish the PPI network of the DEPs from several significantly enriched signaling pathways. The interaction network suggests that a specific protein may be present in various pathways, while a particular signaling pathway could be modulated by numerous proteins. This PPI network indicates a complicated regulatory relationship between DFS, DEPs, and signaling pathways.
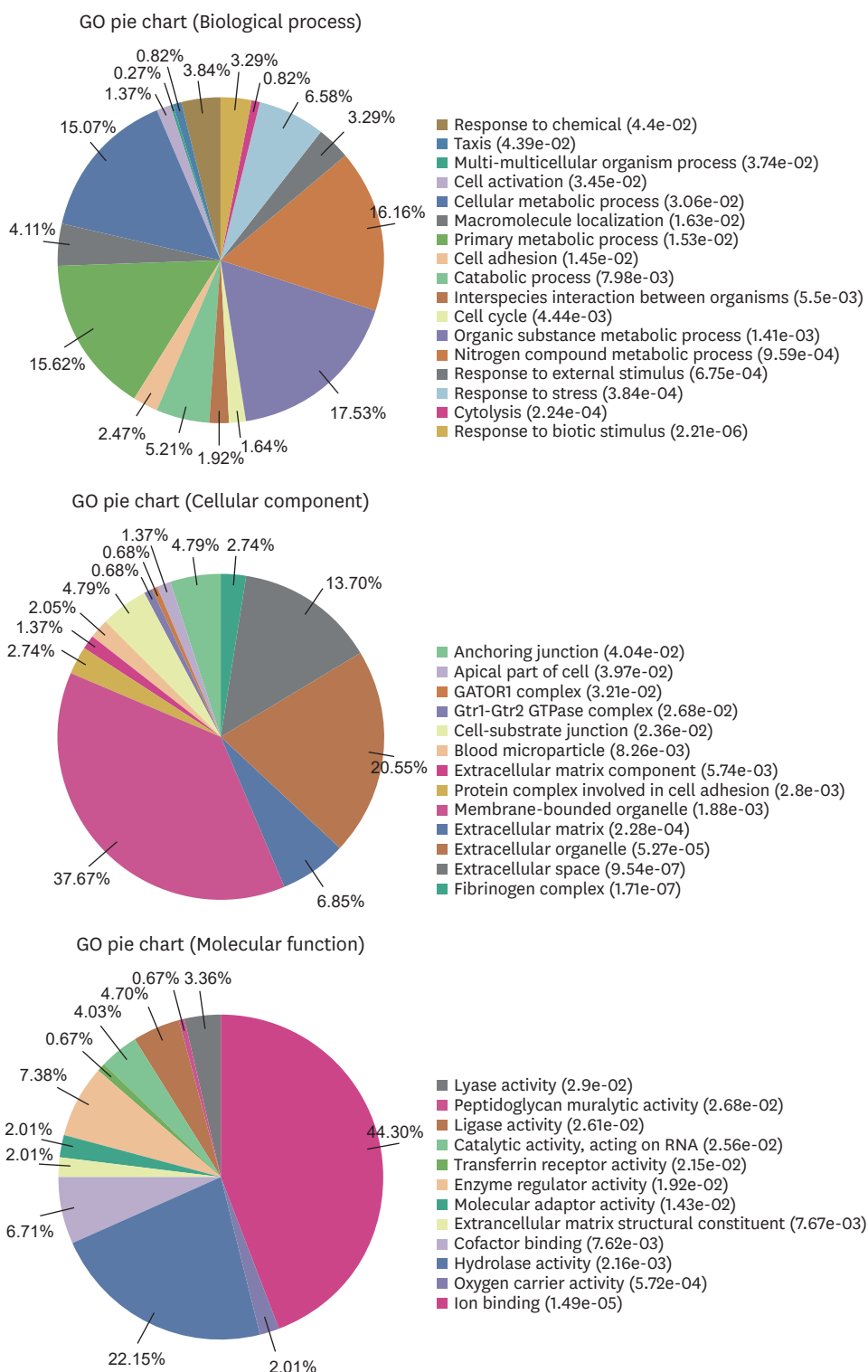
GO pie chart (Biological process)

Response to chemical (4.4e-02)
Taxis (4.39e-02)
Multi-multicellular organism process (3.74e-02)
Cell activation (3.45e-02)
Cellular metabolic process (3.06e-02)
Macromolecule localization (1.63e-02)
Primary metabolic process (1.53e-02)
Cell adhesion (1.45e-02)
Catabolic process (7.98e-03)
Interspecies interaction between organisms (5.5e-03)
Cell cycle (4.44e-03)
Organic substance metabolic process (1.41e-03)
Nitrogen compound metabolic process (9.59e-04)
Response to external stimulus (6.75e-04)
Response to stress (3.84e-04)
Cytolysis (2.24e-04)
Response to biotic stimulus (2.21e-06)

GO pie chart (Cellular component)

Anchoring junction (4.04e-02)
Apical part of cell (3.97e-02)
GATOR1 complex (3.21e-02)
Gtr1-Gtr2 GTPase complex (2.68e-02)
Cell-substrate junction (2.36e-02)
Blood microparticle (8.26e-03)
Extracellular matrix component (5.74e-03)
Protein complex involved in cell adhesion (2.8e-03)
Membrane-bounded organelle (1.88e-03)
Extracellular matrix (2.28e-04)
Extracellular organelle (5.27e-05)
Extracellular space (9.54e-07)
Fibrinogen complex (1.71e-07)

GO pie chart (Molecular function)

Lyase activity (2.9e-02)
Peptidoglycan muralytic activity (2.68e-02)
Ligase activity (2.61e-02)
Catalytic activity, acting on RNA (2.56e-02)
Transferrin receptor activity (2.15e-02)
Enzyme regulator activity (1.92e-02)
Molecular adaptor activity (1.43e-02)
Extrancellular matrix structural constituent (7.67e-03)
Cofactor binding (7.62e-03)
Hydrolase activity (2.16e-03)
Oxygen carrier activity (5.72e-04)
Ion binding (1.49e-05)

Fig. 6. GO classification results. These pie charts demonstrate the proportion of the number of DEPs in each term under their category.
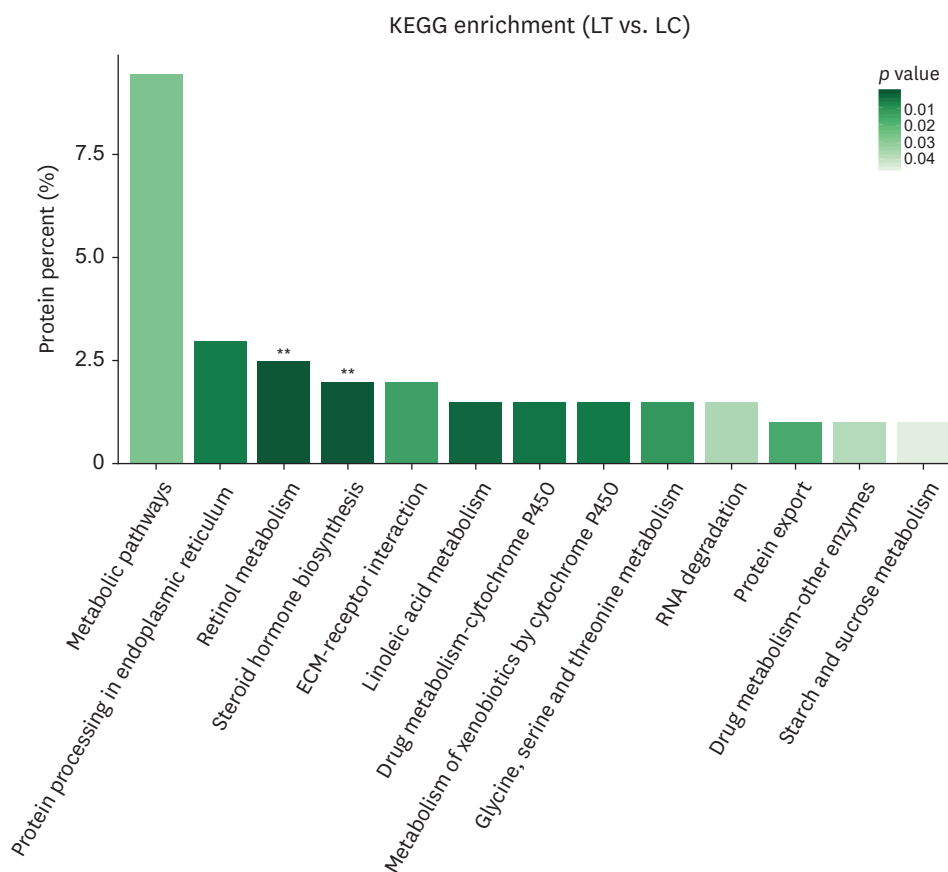GO, Gene Ontology; DEP, differentially expressed protein.

Fig. 7. KEGG pathway enrichment results. The horizontal coordinate indicates different pathways, and the vertical coordinate denotes the number of DEPs in each pathway as a percentage of total DEPs. Deeper color means smaller corrected p value.
KEGG, Kyoto Encyclopedia of Genes and Genomes; DEP, differentially expressed protein; LT, livers from treated group; LC, livers from control group; ECM, extracellular matrix.
*p < 0.05, **p < 0.01.

Verification of the proteomic results

Nine DEPs were selected from **Table 3** for qRT-PCR validation, as presented in **Fig. 9**. Compared to the control group, the mRNA transcript levels of *CYP3A5* (p < 0.01), *HSPA5* (p < 0.01) and *CALR* (p < 0.05) were up-regulated significantly, while *STUB1* (p < 0.01), *CYP3A4* (p < 0.05), *TDH* (p < 0.01), LOC101747660 (p < 0.01), glycine amidinotransferase (GATM; p < 0.01), and CYP2C45 (p < 0.01) was down-regulated significantly. Thus, the results of qRT-PCR validation are consistent with proteomics data.

DISCUSSION

The toxicity symptoms of different avian species resulting from DFS poisoning are similar, while the disparity is only the severity [21,22]. Previous research suggested that the liver is one of the major damaged organs [11,18,23], which has been further confirmed by the serum biochemical results, histopathological analysis, and the expression of apoptosis-related genes in this study. Thus, the liver was chosen as one of the target organs for examining the toxic mechanism of DFS in broiler chickens. Compared to other proteomics techniques, iTRAQ technology has been applied widely in the occurrence and progression mechanism or the search for biomarkers of various diseases with high sensitivity, wide detection range, and
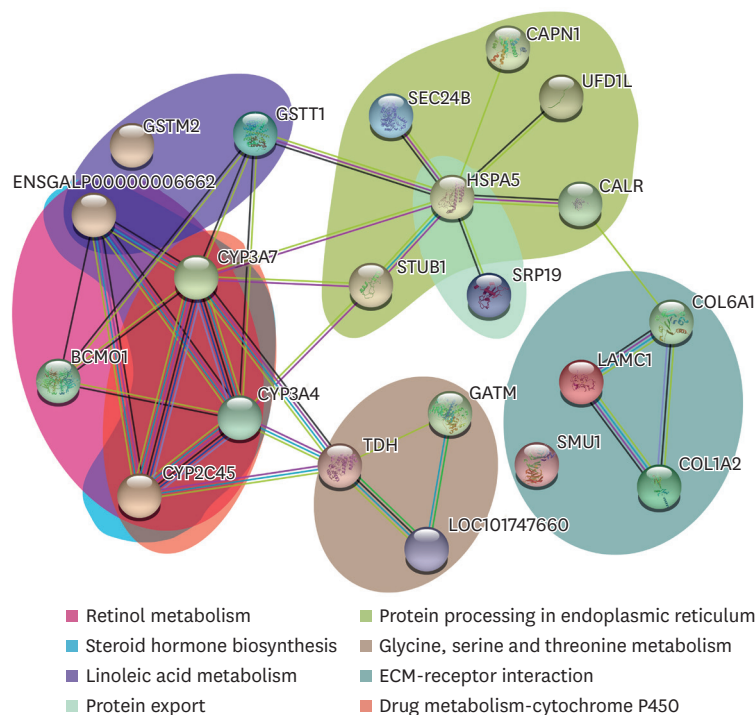
Fig. 8. PPI network of the DEPs. These signaling pathways are distinguished by their distinct colors, and the various nodes indicate the individual DEPs.
PPI, protein-protein interaction; DEP, differentially expressed protein; ECM, extracellular matrix.

Table 3. List of the screened DEPs after DFS administration

Accession	Protein name	Gene name	Fold change	*p* value
F1NT18	Cytochrome P450 3A5	CYP3A5	+2.23	0.001035142
Q90593	Endoplasmic reticulum chaperone BiP	HSPA5	+1.21	0.003515604
A0A1D5P0U5	Calreticulin	CALR	+1.20	0.018197009
P00789	Calpain-1 catalytic subunit	CAPN11	−1.20	0.027542287
F1P1M1	UDP-glucuronosyltransferase	UGT1A1	−1.21	0.011117317
Q9I993	Beta beta-carotene 15,15'-dioxygenase	BCO1	−1.22	0.00311889
Q5ZHY5	STIP1 homology and U box-containing protein 1	STUB1	−1.24	0.047424199
Q98UC3	Ubiquitin fusion-degradation 1-like protein	Ufd1l	−1.24	0.001896706
A0A1D5PCR2	Protein transport protein Sec24B	SEC24B	−1.26	0.042854852
E1BVB6	Cytochrome P450 3A4	CYP3A4	−1.30	0.030269134
F1NFM2	Epimerase domain-containing protein	TDH	−1.33	0.02618183
R4GII9	Beta_elim_lyase domain-containing protein	LOC101747660	−1.33	0.049773708
F1NXN3	Glycine amidinotransferase	GATM	−1.44	0.035237087
A0A1D5PKQ8	Cytochrome P450 2C45	CYP2C45	−2.76	0.001990673

DEP, differentially expressed protein; DFS, diclofenac sodium.
Plus and minus values of fold change represent the up- and down-regulated alteration trend of DEPs, respectively.

good repeatability [15,16]. To select the target DEPs associated with the hepatotoxic effects of DFS, GO and KEGG enrichment analysis was performed, and a PPI network was then established using the STRING database. According to the proteomic results and relevant literature, some pathways were selected as the focal points of the analysis.

Programmed cell death (apoptosis) is a universal form of death regulated by genes, which is crucial for normal organismal development and homeostasis [19]. The intrinsic and extrinsic pathways are the two primary signaling pathways inducing apoptosis. In the
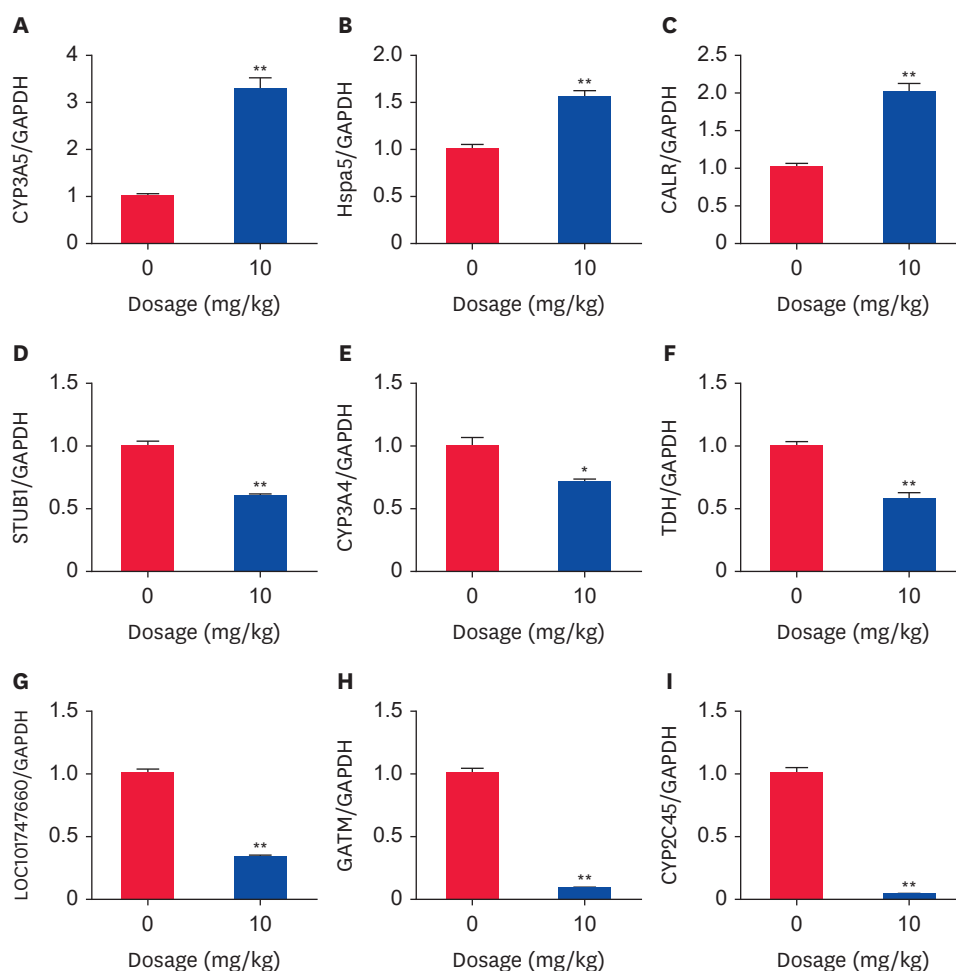
Fig. 9. mRNA transcript levels of screened DEPs in the liver after DFS administration. Data are presented as mean ± SEM.
DEP, differentially expressed protein; SEM, standard error of the mean; GAPDH, glyceraldehyde-3-phosphate dehydrogenase.
*$p < 0.05$, **$p < 0.01$.

intrinsic pathway, activation of the caspase cascade in the cytosol was accomplished through various pro-apoptotic proteins released from different organelles or induced expression of those genes encoding pro-apoptotic proteins. The external pathway was mediated by the interaction between the pro-apoptotic molecules and cell surface receptors to activate the caspase cascade in the cytosol. Hence, it is also referred to as the "death receptor pathway" [20]. Previous studies have shown that DFS can induce apoptosis through multiple routes. In human hepatocytes, diclofenac induces apoptosis by inhibiting mitochondrial respiration [24]. A previous study suggested that diclofenac could also induce human intestinal Caco-2 cell death via endoplasmic reticulum stress and mitochondrial dysfunction [25]. Diclofenac led to a significant increase in death ligand-mediated apoptosis in squamous cell carcinoma cells [26]. In the present study, some DEPs were enriched in the "protein processing in endoplasmic reticulum" signaling pathway, suggesting that the hepatotoxicity of DFS may be achieved by inducing hepatocyte apoptosis through the endoplasmic reticulum pathway. On the other hand, Yamazaki et al. [27] stated that diclofenac can suppress the apoptosis of human neuroblastoma SHSY5Y cells induced by the endoplasmic reticulum, indicating that an intensive investigation is needed to explain the hepatotoxicity mechanism of DFS in terms of inducing apoptosis.

Retinol (vitamin A), a fat-soluble vitamin, is converted to retinaldehyde and retinoic acid in the liver to maintain the normal physiological functions, such as growth, vision, immunity, and antioxidation [28-30]. Retinol and its derivatives can improve the capabilities of antioxidation and scavenging free radicals to reduce the risk of inflammation and oxidative stress [31]. For bovine mammary epithelial cells, a retinol pretreatment attenuated the oxidative injury induced by NO, while the pretreatment with retinoic acid reduced oxidative stress induced by H_2O_2 [32, 33]. Jiang et al. [34] reported that all-trans-retinoic acid could increase the superoxide dismutase activity and glutathione level while reducing the malondialdehyde content in common bile duct ligation rat liver by restoring retinol and retinoic acid contents, and ultimately relieve liver injury. Certainly, retinol is not always favorable for enhancing antioxidant capacity. Dal-Pizzol et al. [35] reported that high-dose retinol could induce oxidative stress in rat Sertoli cells. In the present work, some DEPs were enriched in the "retinol metabolism" pathway, suggesting that DFS might affect the hepatic antioxidant capacity and hepatotoxicity.

Unlike mammals, nitrogen is eventually excreted in the form of uric acid within avian species because of the absence of the ornithine cycle and the lack of uricase [36,37]. Uric acid is the major ultimate product of the purine metabolism. The primary sites for the endogenous production of uric acid are the liver, kidney, intestine, and muscle [38]. De novo synthesis and salvage synthesis are two pathways to produce purine nucleotides. The precursors of the purine ring were determined using an isotope tracer technique: aspartic acid, glutamine, glycine, CO_2, and one-carbon unit [39,40]. The "Glycine, serine, and threonine metabolism" pathway was one of the most significantly enriched pathways in the present study, which was also enriched in a previous study on the nephrotoxicity of DFS on broiler chickens [14]. In the above two studies, GATM was selected as the target DEP and showed a down-regulation trend, highlighting its special status. The liver and kidney are the sites for uric acid synthesis, and glycine is involved in uric acid production. Hence, this pathway can be considered a focus of further research.

Through an analysis of the proteomic results, signaling pathways enriched by DEPs and the complex network connections among them were revealed, all of which may be related to the hepatotoxicity of DFS to broilers. More in-depth studies will be needed on these DEPs and pathways in subsequent work.

In conclusion, DFS administration caused noticeable damage to the liver of broiler chickens, indicating that the liver is one of the main sites of its toxicity. The DEPs and their enriched signaling pathways were screened by proteomic analysis. The hepatotoxicity of DFS on broiler chickens might be achieved by inducing liver cell apoptosis and affecting the metabolism of retinol and purine. The present study could provide molecular insights into the hepatotoxicity of DFS on broiler chickens while also providing a reference for developing more effective and much safer NSAIDs for birds.

REFERENCES

1. Ertekin T, Bilir A, Aslan E, Koca B, Turamanlar O, Ertekin A, et al. The effect of diclofenac sodium on neural tube development in the early stage of chick embryos. Folia Morphol (Warsz). 2019;78(2):307-313.
   PUBMED | CROSSREF

2. Bertocchi P, Antoniella E, Valvo L, Alimonti S, Memoli A. Diclofenac sodium multisource prolonged release tablets--a comparative study on the dissolution profiles. J Pharm Biomed Anal. 2005;37(4):679-685.
    PUBMED | CROSSREF

3. Gan TJ. Diclofenac: an update on its mechanism of action and safety profile. Curr Med Res Opin. 2010;26(7):1715-1731.
    PUBMED | CROSSREF

4. Sharma S, Setia H, Toor AP. Assessing the bioremediation potential of indigenously isolated *Klebsiella* sp. WAH1 for diclofenac sodium: optimization, toxicity and metabolic pathway studies. World J Microbiol Biotechnol. 2021;37(2):33.
    PUBMED | CROSSREF

5. Menassé R, Hedwall PR, Kraetz J, Pericin C, Riesterer L, Sallmann A, et al. Pharmacological properties of diclofenac sodium and its metabolites. Scand J Rheumatol Suppl. 1978;7(22):5-16.
    PUBMED | CROSSREF

6. Swan GE, Cuthbert R, Quevedo M, Green RE, Pain DJ, Bartels P, et al. Toxicity of diclofenac to *Gyps* vultures. Biol Lett. 2006;2(2):279-282.
    PUBMED | CROSSREF

7. Green RE, Taggart MA, Das D, Pain DJ, Sashi Kumar C, Cunningham AA, et al. Collapse of Asian vulture populations: risk of mortality from residues of the veterinary drug diclofenac in carcasses of treated cattle. J Appl Ecol. 2006;43(5):949-956.
    CROSSREF

8. Oaks JL, Gilbert M, Virani MZ, Watson RT, Meteyer CU, Rideout BA, et al. Diclofenac residues as the cause of vulture population decline in Pakistan. Nature. 2004;427(6975):630-633.
    PUBMED | CROSSREF

9. Galligan TH, Mallord JW, Prakash VM, Bhusal KP, Alam AS, Anthony FM, et al. Trends in the availability of the vulture-toxic drug, diclofenac, and other NSAIDs in South Asia, as revealed by covert pharmacy surveys. Bird Conserv Int. 2021;31(3):337-353.
    CROSSREF

10. Paudel K, Amano T, Acharya R, Chaudhary A, Baral HS, Bhusal KP, et al. Population trends in Himalayan Griffon in Upper Mustang, Nepal, before and after the ban on diclofenac. Bird Conserv Int. 2016;26(3):286-292.
    CROSSREF

11. Hussain I, Khan MZ, Khan A, Javed I, Saleemi MK. Toxicological effects of diclofenac in four avian species. Avian Pathol. 2008;37(3):315-321.
    PUBMED | CROSSREF

12. Naidoo V, Swan GE. Diclofenac toxicity in Gyps vulture is associated with decreased uric acid excretion and not renal portal vasoconstriction. Comp Biochem Physiol C Toxicol Pharmacol. 2009;149(3):269-274.
    PUBMED | CROSSREF

13. Nethathe B, Chipangura J, Hassan IZ, Duncan N, Adawaren EO, Havenga L, et al. Diclofenac toxicity in susceptible bird species results from a combination of reduced glomerular filtration and plasma flow with subsequent renal tubular necrosis. PeerJ. 2021;9:e12002.
    PUBMED | CROSSREF

14. Sun C, Lin S, Li Z, Liu H, Liu Y, Wang K, et al. iTRAQ-based quantitative proteomic analysis reveals the toxic mechanism of diclofenac sodium on the kidney of broiler chicken. Comp Biochem Physiol C Toxicol Pharmacol. 2021;249:109129.
    PUBMED | CROSSREF

15. Xie J, Dong W, Liu R, Wang Y, Li Y. Research on the hepatotoxicity mechanism of citrate-modified silver nanoparticles based on metabolomics and proteomics. Nanotoxicology. 2018;12(1):18-31.
    PUBMED | CROSSREF

16. Aslam B, Basit M, Nisar MA, Khurshid M, Rasool MH. Proteomics: technologies and their applications. J Chromatogr Sci. 2017;55(2):182-196.
    PUBMED | CROSSREF

17. Akter R, Sarker M. Effect of diclofenac sodium in broilers. Bangladesh J Vet Med. 2015;13(1):19-24.
    CROSSREF

18. Ramzan M, Ashraf M, Hashmi H, Iqbal Z, Anjum A. Evaluation of diclofenac sodium toxicity at different concentrations in relation to time using broiler chicken model. J Anim Plant Sci. 2015;25(2):357-365.

19. Kannan K, Jain SK. Oxidative stress and apoptosis. Pathophysiology. 2000;7(3):153-163.
    PUBMED | CROSSREF

20. Favaloro B, Allocati N, Graziano V, Di Ilio C, De Laurenzi V. Role of apoptosis in disease. Aging (Albany NY). 2012;4(5):330-349.
    PUBMED | CROSSREF

21. Hassan IZ, Duncan N, Adawaren EO, Naidoo V. Could the environmental toxicity of diclofenac in vultures been predictable if preclinical testing methodology were applied? Environ Toxicol Pharmacol. 2018;64:181-186.
PUBMED | CROSSREF

22. Naidoo V, Duncan N, Bekker L, Swan G. Validating the domestic fowl as a model to investigate the pathophysiology of diclofenac in Gyps vultures. Environ Toxicol Pharmacol. 2007;24(3):260-266.
PUBMED | CROSSREF

23. Cuthbert RJ, Taggart MA, Saini M, Sharma A, Das A, Kulkarni MD, et al. Continuing mortality of vultures in India associated with illegal veterinary use of diclofenac and a potential threat from nimesulide. Oryx. 2016;50(1):104-112.
CROSSREF

24. Goda K, Takahashi T, Kobayashi A, Shoda T, Kuno H, Sugai S. Usefulness of *in vitro* combination assays of mitochondrial dysfunction and apoptosis for the estimation of potential risk of idiosyncratic drug induced liver injury. J Toxicol Sci. 2016;41(5):605-615.
PUBMED | CROSSREF

25. Boonyong C, Vardhanabhuti N, Jianmongkol S. Natural polyphenols prevent indomethacin-induced and diclofenac-induced Caco-2 cell death by reducing endoplasmic reticulum stress regardless of their direct reactive oxygen species scavenging capacity. J Pharm Pharmacol. 2020;72(4):583-591.
PUBMED | CROSSREF

26. Fecker LF, Stockfleth E, Braun FK, Rodust PM, Schwarz C, Köhler A, et al. Enhanced death ligand-induced apoptosis in cutaneous SCC cells by treatment with diclofenac/hyaluronic acid correlates with downregulation of c-FLIP. J Invest Dermatol. 2010;130(8):2098-2109.
PUBMED | CROSSREF

27. Yamazaki T, Muramoto M, Oe T, Morikawa N, Okitsu O, Nagashima T, et al. Diclofenac, a non-steroidal anti-inflammatory drug, suppresses apoptosis induced by endoplasmic reticulum stresses by inhibiting caspase signaling. Neuropharmacology. 2006;50(5):558-567.
PUBMED | CROSSREF

28. Huang Z, Liu Y, Qi G, Brand D, Zheng SG. Role of vitamin A in the immune system. J Clin Med. 2018;7(9):258.
PUBMED | CROSSREF

29. Khillan JS. Vitamin A/retinol and maintenance of pluripotency of stem cells. Nutrients. 2014;6(3):1209-1222.
PUBMED | CROSSREF

30. Tanumihardjo SA, Russell RM, Stephensen CB, Gannon BM, Craft NE, Haskell MJ, et al. Biomarkers of nutrition for development (BOND)-vitamin A review. J Nutr. 2016;146(9):1816S-1848S.
PUBMED | CROSSREF

31. Ford ES, Mokdad AH, Giles WH, Brown DW. The metabolic syndrome and antioxidant concentrations: findings from the Third National Health and Nutrition Examination Survey. Diabetes. 2003;52(9):2346-2352.
PUBMED | CROSSREF

32. Jin L, Yan S, Shi B, Shi H, Guo X, Li J. Retinoic acid attenuates oxidative injury in bovine mammary epithelial cells induced by hydrogen peroxide. Czech J Anim Sci. 2017;62(12):539-548.
CROSSREF

33. Shi HY, Yan SM, Guo YM, Zhang BQ, Guo XY, Shi BL. Vitamin A pretreatment protects NO-induced bovine mammary epithelial cells from oxidative stress by modulating Nrf2 and NF-κB signaling pathways. J Anim Sci. 2018;96(4):1305-1316.
PUBMED | CROSSREF

34. Jiang H, Dan Z, Wang H, Lin J. Effect of ATRA on contents of liver retinoids, oxidative stress and hepatic injury in rat model of extrahepatic cholestasis. J Huazhong Univ Sci Technolog Med Sci. 2007;27(5):491-494.
PUBMED | CROSSREF

35. Dal-Pizzol F, Klamt F, Benfato MS, Bernard EA, Moreira JC. Retinol supplementation induces oxidative stress and modulates antioxidant enzyme activities in rat Sertoli cells. Free Radic Res. 2001;34(4):395-404.
PUBMED | CROSSREF

36. Borghi C, Virdis A. Serum urate, uricase, and blood pressure control in gout. Hypertension. 2019;74(1):23-25.
PUBMED

37. Werner AK, Witte CP. The biochemistry of nitrogen mobilization: purine ring catabolism. Trends Plant Sci. 2011;16(7):381-387.
PUBMED | CROSSREF

38. Maiuolo J, Oppedisano F, Gratteri S, Muscoli C, Mollace V. Regulation of uric acid metabolism and excretion. Int J Cardiol. 2016;213:8-14.
PUBMED | CROSSREF

39. Krebs HA. Regulatory mechanisms in purine biosynthesis. Adv Enzyme Regul. 1977;16:409-422.
   PUBMED | CROSSREF

40. Zhang Y, Morar M, Ealick SE. Structural biology of the purine biosynthetic pathway. Cell Mol Life Sci. 2008;65(23):3699-3724.
   PUBMED | CROSSREF